INTERNATIONAL JOURNAL FOR NUMERICAL METHODS IN FLUIDS, VOL. 16, 287–301 (1993)

INFLUENCE OF PARTICLE DIAMETER DISTRIBUTION ON THE DOWNSTREAM PARTICLE TURBULENCE IN A TWO-PHASE, TURBULENT, ROUND JET

N. P. SARGIANOS, J. S. ANAGNOSTOPOULOS AND G. BERGELES

National Technical University of Athens, Department of Mechanical Engineering, Fluids Section, Laboratory of Aerodynamics, Zografou University Campus, 5, Heroon Polytechniou Street, 15773 Zografou, Athens, Greece

SUMMARY

A numerical algorithm is used to study the 'fan-spreading' mechanism of axial particle turbulence acquisition and the effects on it of the inlet particle diameter distribution, downstream of a particle-laden, turbulent, round jet. The algorithm is based on the particle-source-in-cell numerical technique for two-phase flows. Eulerian equations are used for the description of the gas-phase dynamics, whilst the solid particles are treated within the Lagrangian framework. The turbulent particle dispersion is simulated with the aid of the stochastic separated flow model. It was found that the 'fan-spreading' turbulence is very much affected by the mean and standard deviation of the particle size distribution; in particular, it was found that the 'fan-spreading' mechanism becomes weaker when the standard deviation of the particle diameter distribution is higher and the mean particle diameter smaller. An analytical expression describing the axial particle turbulence due to 'fan-spreading' is proposed and tested, along with a similarity profile valid for the particles of bigger size.

KEY WORDS 'Fan-spreading' Particle turbulence Two-phase flow Turbulent jet Particle-laden jet Numerical study

INTRODUCTION

Two-phase, turbulent, jet flows have been the subject of numerous investigations, both experimental and computational.[1–5] The numerical modelling of such flows is usually based on two different approaches, depending upon the way in which the particulate phase is treated. The Eulerian approach considers the particulate phase to be a continuum which obeys conservation equations similar to those of the gas phase,[6] whereas the Lagrangian approach treats the solid phase in a discrete manner, following the trajectories of a representative number of particles.[7] From published work, it is concluded that flows of low particle mass loading are satisfactorily well represented with the aid of mixed Eulerian/Lagrangian models.

In a recent experimental investigation of a solid-air, turbulent, round jet, laden with large particles,[8] a large anisotropy in particle turbulence (axial to radial particle turbulence ratio 3 : 1) has been observed, albeit the gas-phase turbulence in the same downstream positions did not exhibit such a pronounced anisotropy. In the light of this observation, Hardalupas *et al.*[8] speculated that there is an additional mechanism of particle turbulence acquisition, in addition to that due to the interaction between the gas and particulate phases, which they named 'fan-spreading'. This mechanism was considered to be responsible for the 'fictitious' generation of high

0271–2091/93/040287–15$12.50

Received February 1992
Revised September 1992

axial particle turbulence in the downsteam positions of the jet. The 'fan-spreading' mechanism needs the simultaneous existence of two elements in order to be active: (a) inlet particle radial turbulence, and (b) inlet non-uniform particle velocity profile. If any one of the above two components is missing, then the 'fan-spreading' mechanism of turbulence generation is inactive. It was shown by Mastorakos *et al.*[9] and Sargianos *et al.*[10] that the mixed Eulerian/Lagrangian two-phase flow computer algorithms, which make use of the stochastic separated flow model[11,12] for the simulation of the particulate-phase dispersion, can adequately reproduce the effects of the 'fan-spreading' mechanism in particle-laden, turbulent jets. Furthermore, it was shown by Sargianos *et al.*[10] that there is an upper limit of the inlet radial particle turbulence level, beyond which any increase of its value ceases contributing to the downstream axial particle turbulence intensity via the 'fan-spreading' mechanism. Mastorakos *et al.*[9] and Sargianos *et al.*[10] studied numerically the effects of the 'fan-spreading' mechanism in the case that particles of only one diameter were present; however, in most practical two-phase flow situations there is a distribution of particle diameters, which is usually Gaussian. Therefore, the goal of the present investigation is to identify the influence of the particle diameter distribution on the 'fan-spreading' mechanism, downstream of a particle-laden, turbulent, round jet similar to that of Hardalupas *et al.*[8] For this purpose, an Eulerian/Lagrangian algorithm for two-phase, axisymmetric flows, embodying the stochastic separated flow model for the simulation of particle dispersion, is used. Evaluation of the performance and reliability of the present algorithm can be found in other works.[10,13–15] The numerical experiments to be described and discussed in the present paper refer to particles with Gaussian diameter distribution of mean diameter 30, 100, 200 μm, and standard deviation of 0·1, 0·2, 0·3. Also, comparisons are provided for particles of zero standard deviation.

THEORETICAL ANALYSIS

The mean flow equations

The general form of the time-averaged axisymmetric conservation equations, describing the turbulent motion of the gas phase, is

$$\frac{\partial}{\partial x}(\rho u\Phi)+\frac{1}{r}\frac{\partial}{\partial r}(r\rho v\Phi)=\frac{\partial}{\partial x}\left(\Gamma_\varphi\frac{\partial\Phi}{\partial x}\right)+\frac{1}{r}\frac{\partial}{\partial r}\left(r\Gamma_\varphi\frac{\partial\Phi}{\partial r}\right)+S_\varphi+S_{\mathrm{p},\varphi}, \tag{1}$$

where for $\Phi=1$ the above relation is the continuity equation, for $\Phi=u, v, w$ it gives the three momentum equations and for $\Phi=k, \varepsilon$ it results in the transport equations of the turbulent kinetic energy (k) and its dissipation rate (ε). Expressions for the turbulent diffusivity Γ_φ and the source terms S_φ are given in Table I. The source terms $S_{\mathrm{p},\varphi}$ represent the contribution of the solid-phase momentum changes on the gas-phase momentum, and are of the form (x-direction, for example):

$$S_{\mathrm{p},\varphi}=\dot{m}_\mathrm{p}[(u_{\mathrm{p,in}}-u_{\mathrm{p,out}})+g(1-\rho/\rho_\mathrm{p})(t_\mathrm{in}-t_\mathrm{out})]. \tag{2}$$

The subscripts 'in' and 'out' refer to the time instants that a particle enters or leaves a control volume, respectively. Based on the 'k–ε' turbulence model, an effective viscosity is computed in terms of the following relation:

$$\mu_\mathrm{eff}=\mu_\mathrm{L}+C_\mu\rho k^2/\varepsilon. \tag{3}$$

Particle trajectories

The Lagrangian equations of motion of the particulate phase are

$$\mathrm{d}u_\mathrm{p}/\mathrm{d}t=A(u_\mathrm{g}-u_\mathrm{p})+g, \tag{4}$$

Table I. Turbulent diffusivities and source terms of equation (1), and constants of the '$k-\varepsilon$' turbulence model

Φ	Γ_φ	S_φ
1	0	0
u	μ_{eff}	$-\frac{\partial p}{\partial x}+\frac{\partial}{\partial x}\left(\mu_{\text{eff}}\frac{\partial u}{\partial x}\right)+\frac{1}{r}\frac{\partial}{\partial r}\left(r\mu_{\text{eff}}\frac{\partial v}{\partial x}\right)$
v	μ_{eff}	$-\frac{\partial p}{\partial r}+\frac{\partial}{\partial x}\left(\mu_{\text{eff}}\frac{\partial u}{\partial r}\right)+\frac{1}{r}\frac{\partial}{\partial r}\left(r\mu_{\text{eff}}\frac{\partial v}{\partial r}\right)+\frac{\rho w^2}{2}-2\mu_{\text{eff}}\frac{v}{r^2}$
w	μ_{eff}	$-w\left(\frac{\rho v}{r}+\frac{\mu_{\text{eff}}}{r^2}+\frac{1}{r}\frac{\partial \mu_{\text{eff}}}{\partial r}\right)$
k	$\frac{\mu_{\text{eff}}}{\sigma_k}$	$G-\rho\varepsilon$
ε	$\frac{\mu_{\text{eff}}}{\sigma_\varepsilon}$	$\varepsilon/k(C_1G-C_2\rho\varepsilon)$

$$G=\mu_{\text{eff}}\left[2\left\{\left(\frac{\partial u}{\partial x}\right)^2+\left(\frac{\partial v}{\partial r}\right)^2+\left(\frac{v}{r}\right)^2\right\}+\left(\frac{\partial w}{\partial x}\right)^2+\left(\frac{\partial u}{\partial r}+\frac{\partial v}{\partial x}\right)^2+\left(\frac{\partial w}{\partial r}-\frac{w}{r}\right)^2\right]$$

$C_\mu=0{\cdot}09$, $C_1=1{\cdot}44$, $C_2=1{\cdot}87$, $\sigma_k=0{\cdot}9$, $\sigma_\varepsilon=1{\cdot}3$

$$\mathrm{d}v_{\text{p}}/\mathrm{d}t=A(v_{\text{g}}-v_{\text{p}})+w_{\text{p}}^2/r, \tag{5}$$

$$\mathrm{d}w_{\text{p}}/\mathrm{d}t=A(w_{\text{g}}-w_{\text{p}})-v_{\text{p}}w_{\text{p}}/r, \tag{6}$$

$$\mathrm{d}\mathbf{S}_{\text{p}}/\mathrm{d}t=\mathbf{U}_{\text{p}}, \tag{7}$$

where

$$A=\frac{3}{4}\frac{\mu_{\text{L}}}{\rho_{\text{p}}D_{\text{p}}^2}C_{\text{D}}Re_{\text{p}}. \tag{8}$$

The particle Reynolds number is

$$Re_{\text{p}}=\rho|\mathbf{U}_{\text{g}}-\mathbf{U}_{\text{p}}|D_{\text{p}}/\mu_{\text{L}}. \tag{9}$$

In the above relations, the subscripts p and g denote instantaneous particle- and gas-phase quantities, respectively. The drag coefficient C_{D} is computed according to Wallis:[16]

$$C_{\text{D}}=(1+0{\cdot}15\,Re_{\text{p}}^{0{\cdot}687})/(Re_{\text{p}}/24)\quad\text{for } Re_{\text{p}}\leqslant 1000, \tag{10}$$

$$C_{\text{D}}=0{\cdot}44\quad\text{for } Re_{\text{p}}>1000. \tag{11}$$

The stochastic model of particle dispersion assumes that the flow field is comprised of eddies, whose characteristic length (L_{e}) and lifetime (T_{e}) are

$$L_{\text{e}}=C_\mu^{3/4}k^{3/2}/\varepsilon, \tag{12}$$

$$T_{\text{e}}=L_{\text{e}}/(2k/3)^{1/2}. \tag{13}$$

Every particle interacts with an eddy until the eddy lifetime is terminated or until the particle gets out of the eddy, whichever happens faster. The instantaneous air velocities, appearing in equations (4)–(6), are calculated randomly, assuming that the velocity fluctuations follow Gaussian distribution with standard deviation[12] $\sigma=(2k/3)^{1/2}$.

COMPUTATIONAL DETAILS

The gas-phase equations are discretized with the aid of the 'control volume' method. Discretization is achieved using finite differences and the 'hybrid' differencing scheme, which combines upwind and central differences, depending upon the local mesh Peclet number; then the finite difference equations of the gas phase are solved iteratively using the SIMPLE algorithm.[17,18] After convergence of the gas-phase equations without the presence of the particulate phase, the particles are injected into the converged flow field and, during the integration of their motion, the source terms, which represent the contribution of the discrete phase to the gas-phase equations, are calculated and stored. Then, the gas-phase equations are solved again, including now the previously found particle source terms. This procedure is repeated until final convergence. Convergence is accomplished when the particle source terms and the gas-phase quantities remain almost unchanged between two consecutive iterations. More details and a discussion about the above numerical technique, known as the Particle-Source-In-Cell (PSI-Cell) method, are reported by Crowe *et al.*[19]

All computations reported in this work have been performed on a 386-Weitek computer, working under DOS operating system. A 30×30 non-uniform grid has been utilized to cover the near field of the half jet solved. This size of grid produced predictions which are in close agreement with the measurements of Hardalupas *et al.*,[8] as this is discussed elsewhere.[10,15] The speed of execution was 30 iterations per minute for the computation of the gas-phase equations, and approximately 95 particle trajectories per minute. A total of 20 000 particles, injected from 28 different injection positions, were calculated for each one of the cases discussed in this work.

THE NUMERICAL EXPERIMENTS

The two-dimensional Eulerian/Lagrangian computer code utilized in this study has been used in the past to predict various two-phase flows in simple and complex geometries with encouraging results. Its performance and reliability have been assessed and discussed elsewhere.[10,13–15] Numerical computations are reported in this work for a particle-laden, turbulent, round jet with diameter 15 mm and mean inlet velocity 13 m/s, similar to that used in the measurements of Hardalupas *et al.*[8] A sketch of the jet with the co-ordinate system appears in Figure 1. Particles of mean diameter 30,100 and 200 μm were considered, with density 2000 kg/m. The particles were assumed to follow Gaussian diameter distribution with standard deviations 0·0 (viz. particles of

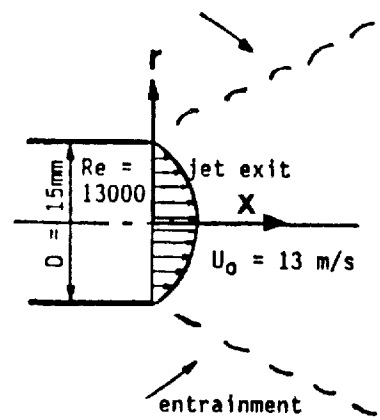

Figure 1. Sketch of the two-phase jet, along with the co-ordinate system used

a single diameter), 0·1, 0·2 and 0·3. The inlet mean particle velocity profile at the pipe exit has been assumed parabolic (the same with the gas phase), and the concentration of particles per unit area at the jet exit constant. Entrainment boundary conditions have been used for the jet edge, whilst at the axis of symmetry the gradient of all quantities has been taken as zero, except for V-velocity, for which $V=0$. The inlet particle axial turbulence was assumed to be zero ($u'_{p_0}=0{\cdot}0$) and the radial particle fluctuating velocity $v'_{p_0}=0{\cdot}05U_0$, where U_0 is the mean axial velocity at the jet centreline. A number of 20,000 particles was used in the calculations in order to produce statistically correct ensemble averages over all particles arriving even at the most remote downstream positions.

RESULTS AND DISCUSSION

Figure 2(a)–2(c) presents the radial profiles of axial particle turbulence at three axial stations 10, 20 and 30 diameters downstream of the jet exit when there are: (a) particles of only one diameter ($D_p=100$ μm) with uniform or parabolic inlet particle velocity profile and (b) particles with Gaussian diameter distribution whose mean diameter is 100 μm and their inlet velocity profile is uniform or parabolic. It is observed that even though the particles are injected from the jet exit with zero inlet axial turbulence, they acquire axial turbulence farther downstream. Clearly, when their inlet velocity profile is uniform, the downstream axial particle turbulence is acquired via the interaction with the gas phase. The particles with Gaussian diameter distribution and uniform inlet velocity profile attain turbulence intensities higher than the particles of a single diameter, at the same downstream positions, because the degree of fluid–particle interaction for this case is different; this is due to the fact that the small particles of the distribution interact with the fluid more intensively, compared to bigger particles whose inertia is higher; this fact adds additional turbulence to the particles. It is also observed that particles with a uniform inlet velocity profile have a lower turbulence level than particles with a parabolic inlet velocity profile; in this case additional turbulence is acquired by the particles via the 'fan-spreading' mechanism, which is explained in the following paragraph.

The 'fan-spreading' mechanism

When the inlet particle velocity profile is parabolic instead of uniform, it is seen that there is an additional increase in the axial particle turbulence intensity downstream of the jet exit, which suggests that there exists another mechanism of particle turbulence generation, termed by Hardalupas *et al.*[8] as 'fan-spreading'. This mechanism can be explained with the aid of the sketch of Figure 3. If radial particle fluctuations exist at two different points of the jet exit, then the particles coming from these points will spread out over some 'fan-like' region. The particles arriving at a downstream position (I) will carry with them information for their inlet axial velocities from their respective points of injection. In the case of a non-uniform inlet mean axial velocity profile the inlet velocity difference will also be present in the ensemble gathered at the downstream position (I) in the form of axial particle velocity fluctuations, and it will show up as axial particle turbulence. If the inlet particle velocity profile was uniform, then there would not exist any mean axial velocity differences at point (I) to give rise to axial particle turbulence. Therefore, referring to Figure 2(a)–2(c), the difference between the two curves, which correspond to the same category of particles, but to parabolic and uniform inlet particle velocity profiles, represents the axial particle turbulence due to 'fan-spreading'. This difference becomes smaller as the particles move downstream (Figure 2(b)–2(c)), because of longer interaction times with the fluid, which results in 'memory loss' of particle inlet conditions, and consequent damping of the 'fan-spreading' mechanism.

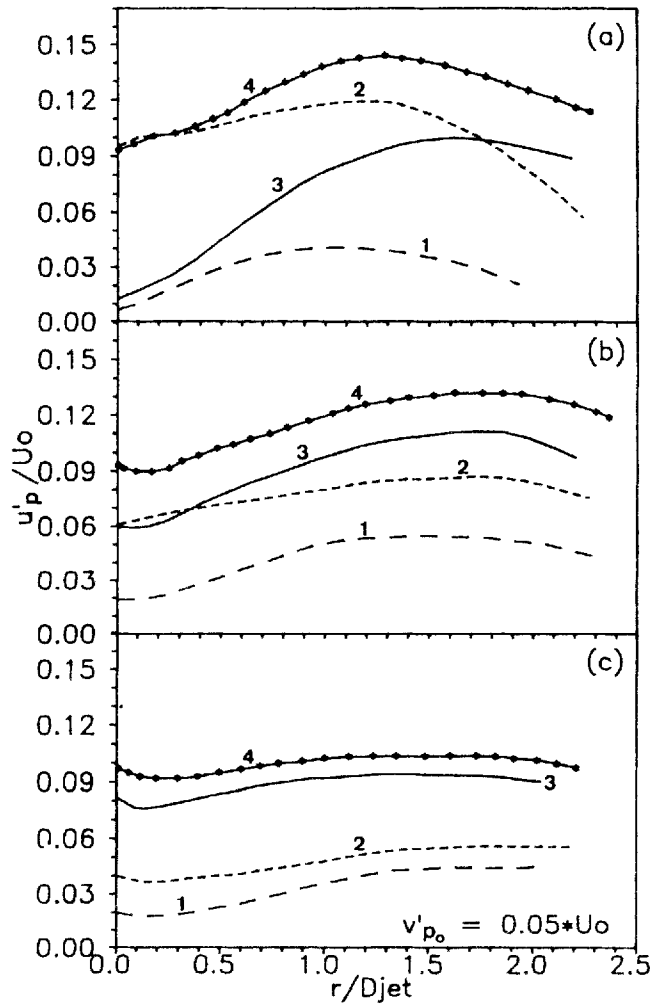

Figure 2. Axial particle turbulence intensity versus radial distance at three downstream stations: (a) at $x=10D$; (b) at $x=20D$; and (c) at $x=30D$, for particles of mean diameter $D_p=100\ \mu m$. (1) $\sigma=0{\cdot}0$, uniform inlet velocity profile; (2) $\sigma=0{\cdot}0$, parabolic inlet velocity profile; (3) $\sigma=0{\cdot}2$, uniform inlet velocity profile; (4) $\sigma=0{\cdot}2$, parabolic inlet velocity profile

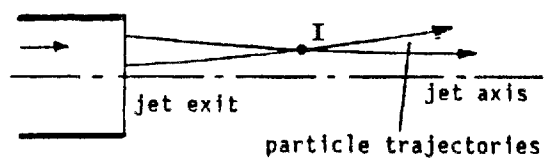

Figure 3. Schematic representation of the 'fan-spreading' mechanism

Trends of 'fan-spreading'

A global view of the 'fan-spreading' axial particle turbulence is shown in the contours of Figure 4(a) (particles with $D_p=100\ \mu m$ and $\sigma=0{\cdot}0$) and of Figure 4(b) (particles with mean diameter 100 μm and $\sigma=0{\cdot}2$). The 'fan-spreading' axial particle turbulence drawn in these figures has been

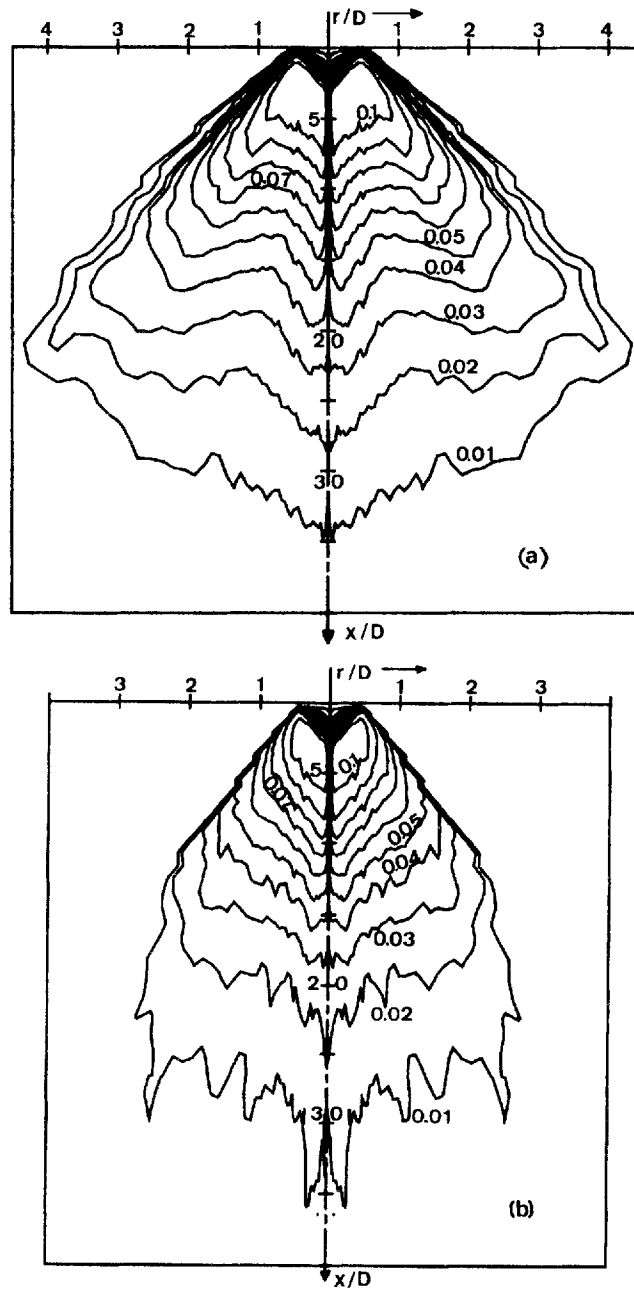

Figure 4. Contours of axial particle turbulence due to 'fan-spreading' for particles of $D_p = 100\ \mu m$; (a) $\sigma = 0{\cdot}0$; (b) $\sigma = 0{\cdot}2$

calculated as the difference in axial particle turbulence between particles of the same size distribution, but with parabolic and uniform inlet velocity profiles. From these contours it is deduced that, for each axial position, the maximum turbulence value due to 'fan-spreading' in the radial direction appears to be near the jet centre line. Also, the 'fan-spreading' becomes weaker with increasing axial distance because far downstream the interaction with the gas phase is

stronger, causing the particles to lose their memory regarding their inlet velocities. It is also seen from the same figures that there is a similarity in the pattern of the contours, axially from a distance bigger than 5 jet diameters away from the jet exit till almost 35 diameters far downstream.

Influence of particle size

In Figure 5(a) and 5(b) analogous results to those described previously, but for the case that the mean particle diameter is now 30 μm, are shown. The same trends are seen again but it is observed that the smaller particles of 30 μm (with Gaussian diameter distribution) tend to exhibit a very low 'fan-spreading' turbulence, even close to their injection position (5 jet diameters downstream, Figure 5(a)), which becomes even smaller farther downstream near the jet axis, and disappears near the jet edge. This can be explained by the fact that the 30 μm particles, having low inertia, are carried away by the fluid and they obtain in very short distances the local gas velocity and turbulence, making the 'fan-spreading' mechanism unimportant. This finding has been also observed experimentally by Hardalupas *et al.*[8] Figure 6 shows the results of computations for particles with mean diameter 200 μm. It is seen that the 'fan-spreading' mechanism is dominant in this case. Comparing Figure 6 with Figures 5(b) and 2(b), one can conclude that the 200 μm particles exhibit the highest 'fan-spreading' turbulence at the same axial positions. This is due to the fact that the 200 μm particles, moving in straight lines due to their high inertia, do not lose their inlet velocity history, and are not affected by their interaction with the gas phase significantly. Hence, the turbulence they obtain through the interaction with the fluid is very low, permitting in this way the 'fan-spreading' to be the main mechanism which controls their

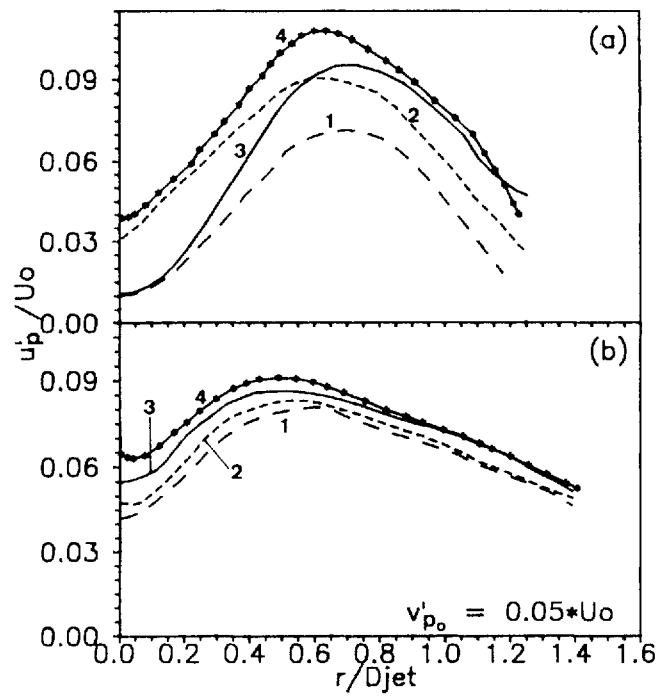

Figure 5. Axial particle turbulence intensity versus radial distance at two downstream stations: (a) at $x = 5D$ and (b) at $x = 10D$, for particles with mean diameter $D_p = 30$ μm. (Legend as in Figure 2)

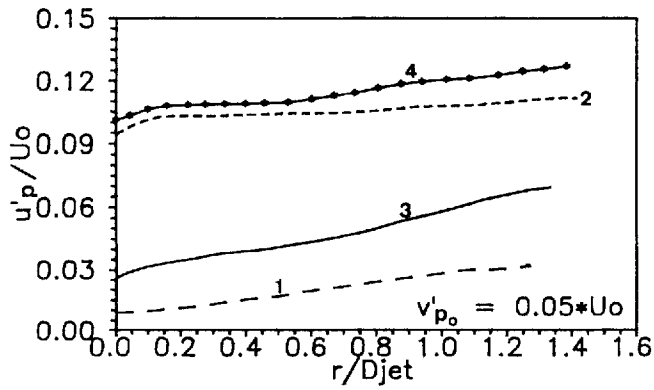

Figure 6. Axial particle turbulence intensity as a function of radial distance at a downstream position $x=20D$, for particles of mean diameter $D_p=200$ μm. (Legend as in Figure 2)

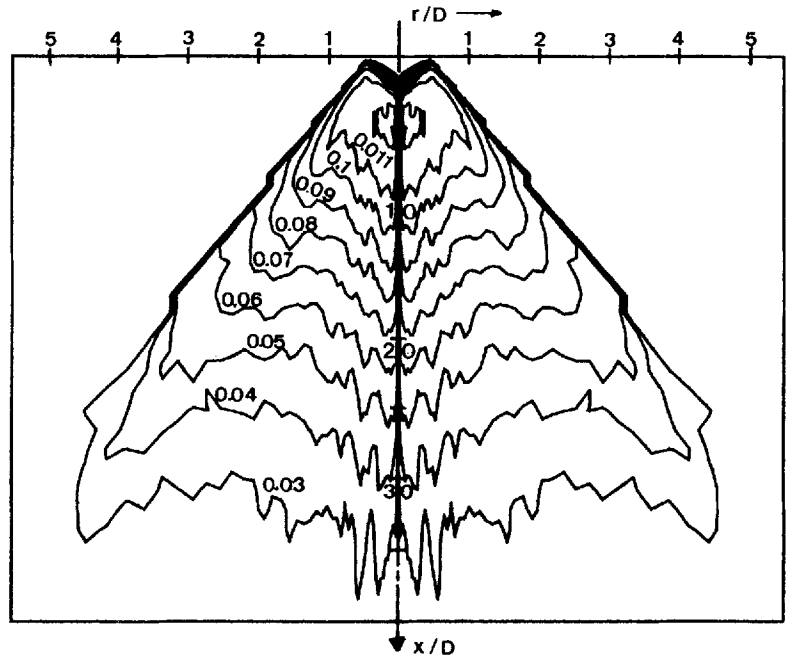

Figure 7. Contours of axial particle turbulence due to 'fan-spreading' for particles of mean diameter $D_p=200$ μm and $\sigma=0{\cdot}2$

turbulence acquisition. In Figure 7 there are contours of the 'fan-spreading' axial particle turbulence for 200 μm particles with standard deviation 0·2. It is observed that for this case too the 'fan-spreading' weakens with axial distance, and along each radial direction it has a maximum value near the jet axis and a minimum value near the jet edge. Figure 8(a) and 8(b) depicts the 'fan-spreading' axial particle turbulence of the three categories of particles examined, when there are particles of a single diameter (Figure 8(a)), and when there is a Gaussian distribution of particle diameters with standard deviation $\sigma=0{\cdot}2$, at an axial distance 20 jet diameters downstream. For both cases, the general conclusion is that the larger the particle size the more influential the 'fan-spreading' mechanism of turbulence generation is.

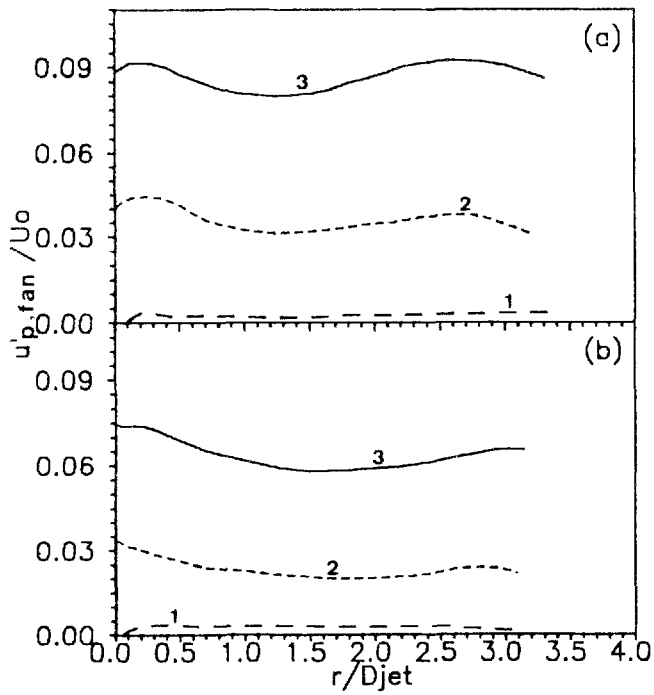

Figure 8. Axial particle turbulence due to 'fan-spreading', as a function of radial distance at a downstream position $x=20D$, for particles of mean diameter $D_p=30\,\mu$m (curve 1), $D_p=100\,\mu$m (curve 2) and $D_p=200\,\mu$m (curve 3), when (a) $\sigma=0{\cdot}0$ and (b) $\sigma=0{\cdot}2$

Influence of standard deviation

Considering particles of normal inlet diameter distribution, and with standard deviations 0·0 (particles of single diameter), 0·1, 0·2 and 0·3, it is concluded from Figure 9(a) and 9(b) that the higher the standard deviation of the particle size distribution used, the lower the 'fan-spreading' turbulence. This can be explained by the fact that the higher the standard deviation, the wider the range of particle diameters participating in the two-phase flow. This means that there is a larger number of smaller particles which interact more intensively with the fluid and, hence, they very quickly attain velocities close to those of the gas phase. Thus, when the trajectories of these smaller particles cross each other, the difference in their mean axial velocities (which shows up as 'fan-spreading' turbulence) is lower than if the crossing particles were all of the same diameter ($\sigma=0{\cdot}0$). When the standard deviation of the particle size distribution is small, then the range of particle diameters is narrow (very close to the mean value) and, consequently, the interaction with the gas phase is almost of the same degree for all particles. This interaction is weaker for $\sigma=0{\cdot}0$ compared to the cases with larger standard deviations. For this reason, these particles preserve even in remote downstream positions the 'memory' of their inlet velocities, which at points of crossing trajectories shows up as high axial particle turbulence due to the 'fan-spreading' mechanism.

Mathematical description of 'fan-spreading'

An effort has been undertaken to describe mathematically the axial particle turbulence due to the 'fan-spreading' mechanism. It has been noted earlier that the 'fan-spreading' turbulence

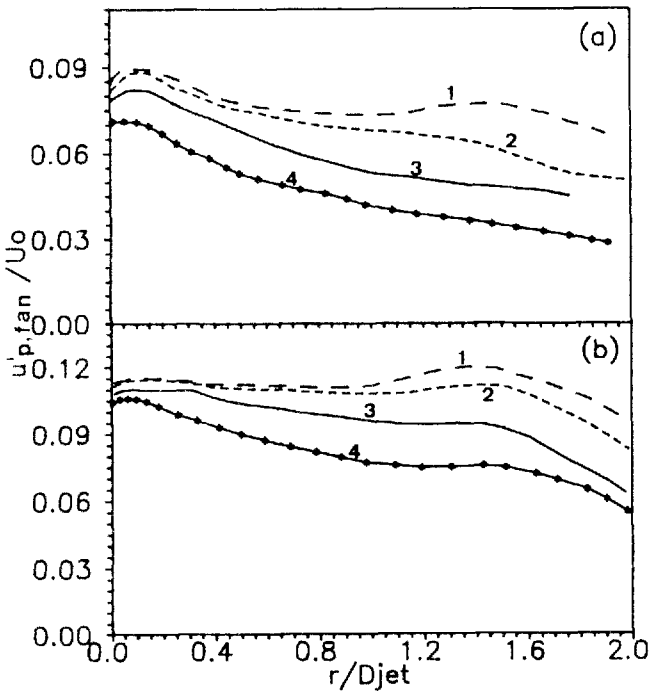

Figure 9. Comparative plots of the 'fan-spreading' axial particle turbulence, at an axial position $x = 10D$ downstream, for various standard deviations of the particle size distribution, when the mean particle diameter is: (a) $D_p = 100\ \mu m$ and (b) $D_p = 200\ \mu m$. {(1) $\sigma = 0{\cdot}0$; (2) $\sigma = 0{\cdot}1$; (3) $\sigma = 0{\cdot}2$; (4) $\sigma = 0{\cdot}3$}

decreases with decreasing mean particle diameter and increasing standard deviation. Therefore, a relation describing the 'fan-spreading' turbulence should be inversely proportional to these quantities and should give a constant value for particles of infinite inertia ($D_p \to \infty$), and an infinite value for very small particles ($D_p \to 0$). Introducing a dimensionless Stokes number (St_e), which characterizes the particle injection conditions at the jet exit, as

$$St_e = \frac{D_{jet}}{U_0 \tau_p}, \tag{14}$$

where D_{jet} is the diameter of the jet, U_0 the mean axial velocity at the jet exit, and τ_p a particle time constant representing the particle inertia, which for heavy particles (that is, particles with a density much higher than that of the gas phase) is defined as[8, 20]

$$\tau_p = \frac{D_p^2 \rho_p}{18 \rho \nu}, \tag{15}$$

then a relation of the form proposed in the following complies with the earlier stated properties of the 'fan-spreading' turbulence and, therefore, might be suitable for the mathematical description of the axial particle turbulence due to the 'fan-spreading' mechanism (u'_{fan}):

$$\log(u'_{fan}/U_0) \approx \frac{A(x/D_{jet})(St_e)^n}{1 - B\sigma(St_e)^m} - C. \tag{16}$$

The coefficients of the above relation (A, B, C, n, m) have been calibrated for values of the 'fan-spreading' on the centreline of the jet and for particles of 200 and 30 μm with standard deviations

0·0 and 0·3. The values of these constants for the 'fan-spreading' turbulence on the jet axis were found to be $A=-8/25$, $B=1/10$, $C=4/5$, $n=3/5$ and $m=-1/2$. Using these values for the constants, and the above proposed relation, the predicted 'fan-spreading' turbulence via the above equation has been compared with that obtained by the two-phase computer code for the 100 μm particles. To test the reliability of the above equation, additional runs of the two-phase algorithm for particles with mean diameter 300, 150 and 65 μm and standard deviation $\sigma=0{\cdot}15$, and also for particles of infinite inertia, were performed. Then the 'fan-spreading' along the jet axis was compared to that found using equation (16) and the previously computed coefficients (Figure 11). As one can see, the agreement is very good in both Figures 10 and 11.

The validity of the above equation is, for axial distances, from 5 to 40 jet diameters downstream, and it holds true for the inlet particle u'_{p_0} and v'_{p_0} used, for the same Re ($Re=13{,}000$) and

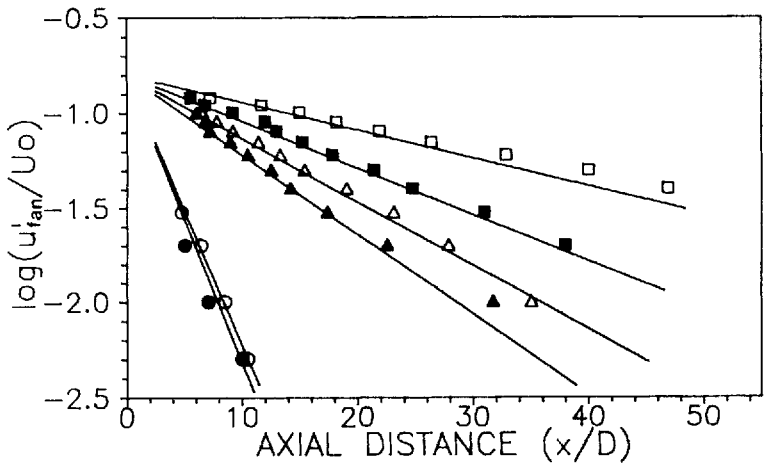

Figure 10. Comparison of the 'fan-spreading' axial particle turbulence on the jet axis, computed via equation (16) (solid lines), to that predicted by the two-phase flow algorithm. □□: $D_p=200$ μm, $\sigma=0{\cdot}0$; △△: $D_p=100$ μm, $\sigma=0{\cdot}0$; ○○: $D_p=30$ μm, $\sigma=0{\cdot}0$; ■■: $D_p=200$ μm, $\sigma=0{\cdot}3$; ▲▲: $D_p=100$ μm, $\sigma=0{\cdot}3$; ●●: $D_p=30$ μm, $\sigma=0{\cdot}3$

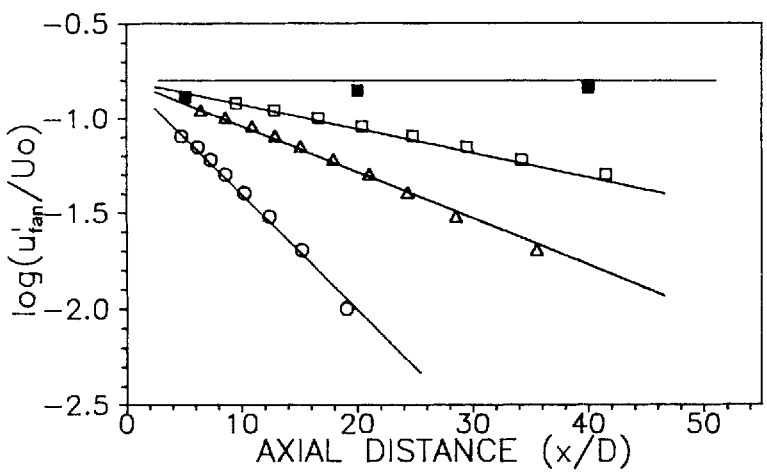

Figure 11. Additional comparisons of the 'fan-spreading' axial particle turbulence on the jet axis, calculated via equation (16) (solid lines), to that predicted by the two-phase flow algorithm. ■■■: particles of infinite inertia; □□□: $D_p=300$ μm, $\sigma=0{\cdot}15$; △△△: $D_p=150$ μm, $\sigma=0{\cdot}15$; ○○○: $D_p=65$ μm, $\sigma=0{\cdot}15$

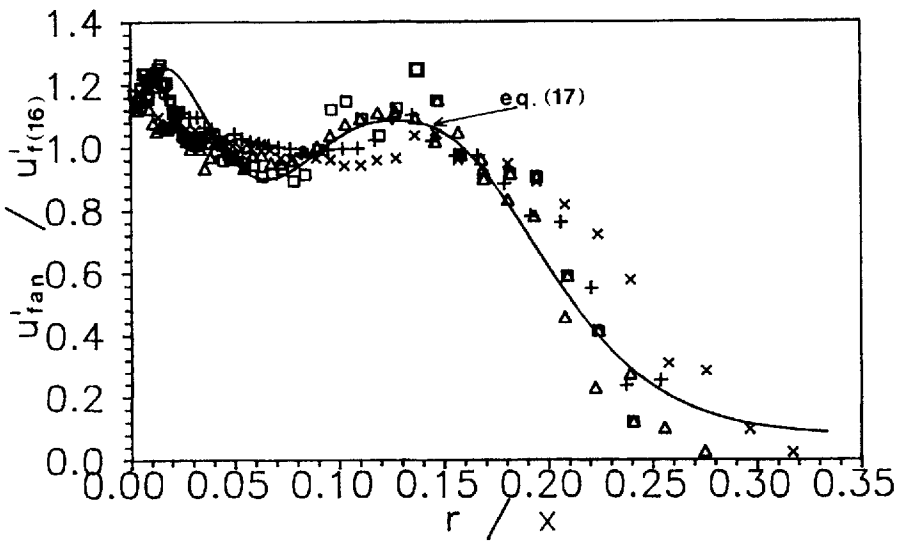

Figure 12. Self-similar profiles of the 'fan-spreading' axial particle turbulence, at several downstream stations, for particles of $D_p = 100\ \mu m$ and $D_p = 200\ \mu m$, calculated by the two-phase algorithm. × × ×: $D_p = 100\ \mu m$, $x = 8D$; + + +: $D_p = 100\ \mu m$, $x = 10D$; △△△: $D_p = 200\ \mu m$, $x = 20D$; □□□: $D_p = 200\ \mu m$, $x = 40D$; —: similarity profile calculated through equation (17)

for an inlet particle velocity profile similar to that of the fluid. It is the authors' feeling though that relations of a similar form might still hold for solid–air flows of different characteristics than those described previously.

Non-dimensionalizing the axial particle 'fan-spreading' turbulence at each axial station by the corresponding value obtained via equation (16), and the radial by the axial distance, the plot of Figure 12 is produced for particles of uniform diameters $D_p = 100\ \mu m$ and $D_p = 200\ \mu m$. It is clear from this figure that this transformation reduces the 'fan-spreading' turbulence profiles to a single profile, despite the scattering of values; this is an indication that there exists profile self-similarity for the large particles with $\sigma = 0{\cdot}0$. The self-similarity of profiles extends farther downstream ($x = 40D$) for the particles with $D_p = 200\ \mu m$, whilst it is substantially delimited upstream ($x = 10D$) for the smaller particles (with $D_p = 100\ \mu m$). This observation is reasonable, since it has been noted earlier that the 'fan-spreading' mechanism is active even far downstream for the bigger particles, whilst for smaller particles it is limited to regions close to the injection point. The similarity of profiles gave rise to an effort for their analytical description; it was found that the self-similar profile can be matched by a curve defined by the following relation (Figure 12):

$$u'_{fan}/u'_{f(16)} \approx \operatorname{sech}^2 \lambda + \operatorname{sech}^2 \xi + Q, \tag{17}$$

where $\lambda = \beta(r/x - \alpha/10)$, $\xi = \delta|r/x - \alpha|^{\gamma}$, $Q = 3/40$, $\alpha = 1/8$, $\beta = 26$, $\gamma = 6/5$ and $\delta = 20$.

The fit of the curve produced via relation (17) to the predicted data of Figure 12 is satisfactory, despite the high degree of scattering of these data. Hyperbolic functions, as those of equation (17), often describe the similarity region of free jets;[21] from this point of view, the form of relation (17) seems to be realistic.

CONCLUSIONS

A computer algorithm for two-phase, axisymmetric flows, embodying the 'Stochastic Separated Flow' (SSF) model for simulating particle dispersion, has been used in this work in order to

identify numerically the influence of the inlet particle diameter distribution and standard deviation on the downstream axial particle turbulence of a particle-laden, turbulent, round jet. Numerical computations have been made for 30, 100 and 200 μm particles with standard deviations 0·0, 0·1, 0·2, and 0·3. It was found that the particles acquire axial turbulence via the interaction with the fluid, and via the 'fan-spreading' mechanism. The 'fan-spreading' turbulence is insignificant for small particles, whereas it is of considerable magnitude for bigger particles, decreasing with an increase of the standard deviation of particle size distribution. Furthermore, it was observed that, at the same downstream position, the 'fan-spreading' mechanism is stronger near the jet axis than near the jet edge. Also, this phenomenon becomes weaker with increasing distance from the jet exit. An analytical expression which estimates the 'fan-spreading' turbulence on the jet axis as a function of particle mean diameter, standard deviation and axial distance has been proposed and tested for several cases with good results. Finally, it was shown that the 'fan-spreading' axial turbulence profiles of the large particles (for monodispersed particles) are self-similar. These self-similar profiles were found to obey an analytical expression involving hyperbolic trigonometric functions, which commonly describe self-preserved velocity profiles of free shear flows.

ACKNOWLEDGEMENT

The financial support of this research by the Commission of the European Communities/D.G.-XII under contract EN3F-022-GR(T-T) is gratefully acknowledged.

REFERENCES

1. G. Hetsroni and M. Sokolov, 'Distribution of mass, velocity, and intensity of turbulence in a two-phase turbulent jet', *ASME J. Appl. Mech.*, **38**, 315–327 (1971).
2. K. Hayashi and M. C. Branch, 'Concentration, velocity and particle measurements in gas–solid, two-phase jets', *J. Energy*, **4**, 193–198 (1980).
3. Y. Levy and F. C. Lockwood, 'Velocity measurements in a particle-laden, turbulent free jet', *Combust. Flame*, **40**, 333–339 (1981).
4. D. Modarress, H. Tan and S. Elghobashi, 'Two-component LDA measurements in a two-phase turbulent jet', *AIAA J.*, **22**, 624–630 (1984).
5. J. S. Shuen, A. S. P. Solomon, Q. F. Zhang and G. M. Faeth, 'Structure of particle-laden jets: measurements and predictions', *AIAA J.*, **23**, 396–404 (1985).
6. S. E. Elghobashi and T. W. Abou-Arab, 'A two-equation turbulence model for two-phase flows', *Phys. Fluids*, **26**, 931–938 (1983).
7. D. Migdal and V. D. Agosta, 'A source flow model for continuum gas-particle flow', *ASME J. Appl. Mech.*, **34**, 860–865 (1967).
8. Y. Hardalupas, A. M. K. P. Taylor and J. H. Whitelaw, 'Velocity and particle-flux characteristics of turbulent particle-laden jets', *Proc. R. Soc. Lond.*, **A426**, 31–78 (1989).
9. F. Mastorakos, J. J. McGuirk and A. M. K. P. Taylor, 'The origin of turbulence acquired by heavy particles in a round, turbulent jet', *Paper presented at the International Conference on Mechanics of Two-Phase Flows*, Taipei, Taiwan, 1989.
10. N. P. Sargianos, J. Anagnostopoulos and G. Bergeles, 'Turbulence modulation of particles downstream of a two-phase, particle-laden round jet', in W. Rodi and E. N. Ganic (eds), *Proc. 1st Int. Symp. on Engineering Turbulence Modelling and Measurements* held in Dubrovnik-Yugoslavia, Elsevier, Amsterdam, 1990, pp. 897–906.
11. A. D. Gosman and S. I. Ioannides, 'Aspects of computer simulation of liquid-fueled combustors', *J. Energy*, **7**, 482–490 (1983).
12. J. S. Shuen, L. D. Chen and G. M. Faeth, 'Evaluation of a stochastic model of particle dispersion in a turbulent round jet', *AIChE J.*, **29**, 167–170 (1983).
13. J. Anagnostopoulos and G. Bergeles, 'Numerical study of particle-laden jets: a Lagrangian approach', in C. M. Brauner and C. Shmidt-Laine (eds), *Mathematical Modelling in Combuston and Related Topics*, NATO ASI Series E (Applied Sciences—No. 140), Martinus Nijhoff, Dordrecht, 1988, pp. 345–354.
14. J. Anagnostopoulos and G. Bergeles, 'Discrete phase effects on the flow field of a droplet-laden swirling jet with recirculation: a numerical study', *Int. J. Heat Fluid Flow* **13**, (2), 141–150 (1992).

15. J. S. Anagnostopoulos, 'Numerical solution of conservation equations for two-phase flow in axisymmetric burners', *Ph.D. Thesis*, Nat. Tech. Univ. of Athens, Athens, Greece, 1991.
16. G. B. Wallis, *One-Dimensional Two-Phase Flow*, McGraw-Hill, New York, 1969, pp. 177–178.
17. S. V. Patankar and D. B. Spalding, 'A calculation procedure for heat, mass and momentum in three-dimensional parabolic flows', *Int. J. Heat Mass Transfer*, **15**, 1787–1806 (1972).
18. S. V. Patankar, *Numerical Heat Transfer and Fluid Flow*, Hemisphere, Washington, DC, 1980.
19. C. T. Crowe, M. P. Sharma and D. E. Stock, 'The particle-source-in-cell method for gas-droplet flow', *ASME J. Fluids Eng.*, **99**, 325–332 (1977).
20. W. H. Snyder and J. L. Lumley, 'Some measurements of particle velocity autocorrelation functions in a turbulent flow', *J. Fluid Mech.*, **48**, 41–71 (1971).
21. F. M. White, *Viscous Fluid Flow*, McGraw-Hill, New York, 1974, pp. 506–508.